

# WormCat: An Online Tool for Annotation and Visualization of *Caenorhabditis elegans* Genome-Scale Data

Amy D. Holdorf,\* Daniel P. Higgins,<sup>†</sup> Anne C. Hart,<sup>‡</sup> Peter R. Boag,<sup>§</sup> Gregory J. Pazour,\*\* Albertha J. M. Walhout,\*<sup>\*\*\*</sup> and Amy K. Walker\*\*<sup>1</sup>

\*Program in Systems Biology, University of Massachusetts Medical School, Worcester, Massachusetts 01605, <sup>†</sup>Department of Computer Science, Georgia Technical University, Atlanta, Georgia 30332-0765, <sup>‡</sup>Department of Neuroscience, Robert J. and Nancy D. Carney Institute for Brain Science, Brown University, Providence, Rhode Island 02912, <sup>§</sup>Department of Biochemistry and Molecular Biology, Monash University, 3800 Clayton Australia, and \*\*Program in Molecular Medicine, University of Massachusetts Medical School, Worcester, Massachusetts 01605

ORCID IDs: 0000-0002-4660-354X (D.P.H.); 0000-0001-7239-4350 (A.C.H.); 0000-0002-0889-0859 (P.R.B.); 0000-0002-6285-8796 (G.J.P.); 0000-0001-5587-3608 (A.J.M.W.); 0000-0003-1899-8916 (A.K.W.)

**ABSTRACT** The emergence of large gene expression datasets has revealed the need for improved tools to identify enriched gene categories and visualize enrichment patterns. While gene ontology (GO) provides a valuable tool for gene set enrichment analysis, it has several limitations. First, it is difficult to graph multiple GO analyses for comparison. Second, genes from some model systems are not well represented. For example, ~30% of *Caenorhabditis elegans* genes are missing from the analysis in commonly used databases. To allow categorization and visualization of enriched *C. elegans* gene sets in different types of genome-scale data, we developed WormCat, a web-based tool that uses a near-complete annotation of the *C. elegans* genome to identify coexpressed gene sets and scaled heat map for enrichment visualization. We tested the performance of WormCat using a variety of published transcriptomic datasets, and show that it reproduces major categories identified by GO. Importantly, we also found previously unidentified categories that are informative for interpreting phenotypes or predicting biological function. For example, we analyzed published RNA-seq data from *C. elegans* treated with combinations of lifespan-extending drugs, where one combination paradoxically shortened lifespan. Using WormCat, we identified sterol metabolism as a category that was not enriched in the single or double combinations, but emerged in a triple combination along with the lifespan shortening. Thus, WormCat identified a gene set with potential phenotypic relevance not found with previous GO analysis. In conclusion, WormCat provides a powerful tool for the analysis and visualization of gene set enrichment in different types of *C. elegans* datasets.

**KEYWORDS** *C. elegans*; gene set enrichment analysis; RNA sequencing visualization

**R**NA-SEQ is an indispensable tool for understanding how gene expression changes during development or upon environmental perturbations. As this technology has become less expensive and more robust, it has become more common to generate data from multiple conditions, enabling

comparisons of gene expression profiles across biological contexts. The most commonly used method to derive information on the biological function of coexpressed genes is gene ontology (GO) (The Gene Ontology Consortium 2019) (Ashburner *et al.* 2000), where annotation for each gene follows three major classifications: *Biological Process*, *Molecular Function*, or *Cellular Component*. For example, the *Biological Process* class refers to genes included in a process that an organism is programmed to execute, and that occurs through specific regulated molecular events. *Molecular Function* denotes protein activities, and *Cellular Component* maps the location of activity. Within each of these classifications, functions are broken down in parent-child relationships with increasing functional

Copyright © 2020 by the Genetics Society of America

doi: <https://doi.org/10.1534/genetics.119.302919>

Manuscript received August 15, 2019; accepted for publication December 2, 2019; published Early Online December 6, 2019.

Available freely online through the author-supported open access option.

Supplemental material available at figshare: <https://doi.org/10.25386/genetics.10312070>.

<sup>1</sup>Corresponding author: Program in Molecular Medicine, University of Massachusetts Medical School, 373 Plantation St., Worcester, MA 01605. E-mail: amy.walker@umassmed.edu

specificity (Figure 1A). However, child classes can be linked to different parent classes, making statistical analysis not straightforward. For example, the child class *phospholipid biosynthetic process* can be linked to both of the parent groupings *metabolic process* and *cellular process*. Thus, GO provides multiple descriptors per gene. Although GO was developed to compare gene function across newly sequenced genomes, it became apparent that it could also be used to identify shared functional classifications within large-scale gene expression data (Eisen *et al.* 1998; Spellman *et al.* 1998). Currently, multiple web-based servers that use different statistical tests can be used to determine the enrichment of GO terms for a gene set of interest. For example, PANTHER ([www.pantherdb.org](http://www.pantherdb.org)) provides enriched GO terms determined by Fisher's Exact Test with a Benjamini-Hochberg false discovery rate (FDR) correction for 131 species (Mi *et al.* 2019). Because the multiplicity of GO term parent-child relationships can produce complex data structures, specialized ontologies such as GO-Slim use a restricted set of terms, searching biological processes as default (Mi *et al.* 2019). *P*-values provide relevance for enriched GO terms. Visualization of gene set enrichment data are important for identifying critical elements and communication of information. PANTHER provides pie or bar charts of individual searches (Mi *et al.* 2019). The GOrilla platform generates tables of *P*-values (Eden *et al.* 2009) and links to another service, REVIGO, that uses semantic graphs to visualize GO terms data (Supek *et al.* 2011). Thus, the GO databases provide a widely used platform for classifying, comparing, and visualizing functional genomic data. However, as outlined below, GO is of limited use for the analysis of *Caenorhabditis elegans* data and visualization of multiplexed datasets.

The nematode *C. elegans* has been at the forefront of genomics research. It was the first metazoan organism with a completely sequenced genome (*Caenorhabditis elegans* Sequencing Consortium 1998). After the discovery of RNA interference (RNAi) (Fire *et al.* 1998), multiple RNAi libraries were developed for performing genome-wide knockdown screens (Kamath *et al.* 2003; Rual *et al.* 2004). Gene expression profiling studies using microarrays or RNA-seq have compared gene expression in sex-specific, developmental/aging-related, specific gene deletion, tissue-specific, and dietary or stress-related animal conditions (Reinke *et al.* 2000; Hillier *et al.* 2005; Baugh *et al.* 2009; Oliveira *et al.* 2009; Deng *et al.* 2011; Schwarz *et al.* 2012; Bulcha *et al.* 2019). While GO has been used extensively to analyze *C. elegans* gene expression profiling data, it has several limitations. First, ~30% of *C. elegans* genes are not annotated in GO databases (Ding *et al.* 2018), excluding these genes from the analysis. Thus, these genes are arbitrarily excluded from enrichment statistics. Second, the visualization of enrichment data from comparative RNA-seq datasets is difficult, and this is true not only for *C. elegans* datasets but for gene expression profile comparisons in any organism. Most users display the output data as lists with *P*-values (MacNeil *et al.* 2013) or as pie or bar charts (Ding *et al.* 2015), which are challenging to multiplex for comparison of multiple datasets. Finally, it can be challenging to

determine which input genes are associated with a given GO classification, which is critical for interpreting the accuracy and biological importance of enriched gene sets.

We constructed a web-based gene set enrichment analysis tool we named WormCat (WormCatalog) that works independently from GO to identify potentially coexpressed or cofunctioning genes in genome-wide expression studies or functional screens. WormCat ([www.wormcat.com](http://www.wormcat.com)), uses a concise list of nested categories where each gene is first assigned to a category based on physiological function, and then to a molecular function or cellular location. WormCat provides a scaled bubble chart that allows the visualization and direct comparison of complex datasets. The tool also provides csv files containing input gene annotations, *P*-values from Fisher's exact tests, and Bonferroni multiple hypothesis testing corrections. We used WormCat to identify functional gene sets in published gene expression data and large-scale RNAi screens. WormCat reproducibly identified prior GO classifications, and provided an easy way to interpret visualization that enables the facile and intuitive comparison of multiple published datasets. We also identified new groups of enriched categories with potentially important biological significance, showing that WormCat provides enrichment information not revealed by GO. Taken together, WormCat offers an alternative and complementary tool for categorizing and visualizing data for genome-wide *C. elegans* studies, and may provide a platform for similar annotations in other model organisms and humans.

## Materials and Methods

### Annotations

WormBase version WS270 was used to provide WormBase descriptions and provide phenotype information.

### Scripts

The processed data were analyzed using R version 3.4.4 (2018-03-15), and depends on the following R packages: datasets, graphics, grDevices, methods, stats, utils, ggplot2, plot flow, scales, ggthemes, pander, data.table, plyr, gdttools, svglite, and FSA.

### Data availability

The authors state that all data necessary for confirming the conclusions presented in the article are represented fully within the article. The code and annotation lists are available under MIT Open Source License, and can be downloaded from the GitHub repository <https://github.com/dphiggs01/wormcat> along with version-control information. Alternatively, WormCat can be installed directly as an R package using the devtools library. Supplemental material has been deposited at figshare and includes 12 supplemental figures and 14 supplemental tables. Supplemental material available at figshare: <https://doi.org/10.25386/genetics.10312070>.

**GO searches:** Genes lists were entered as test sets into GOrilla (<http://cbl-gorilla.cs.technion.ac.il/>) (Eden *et al.* 2009) with

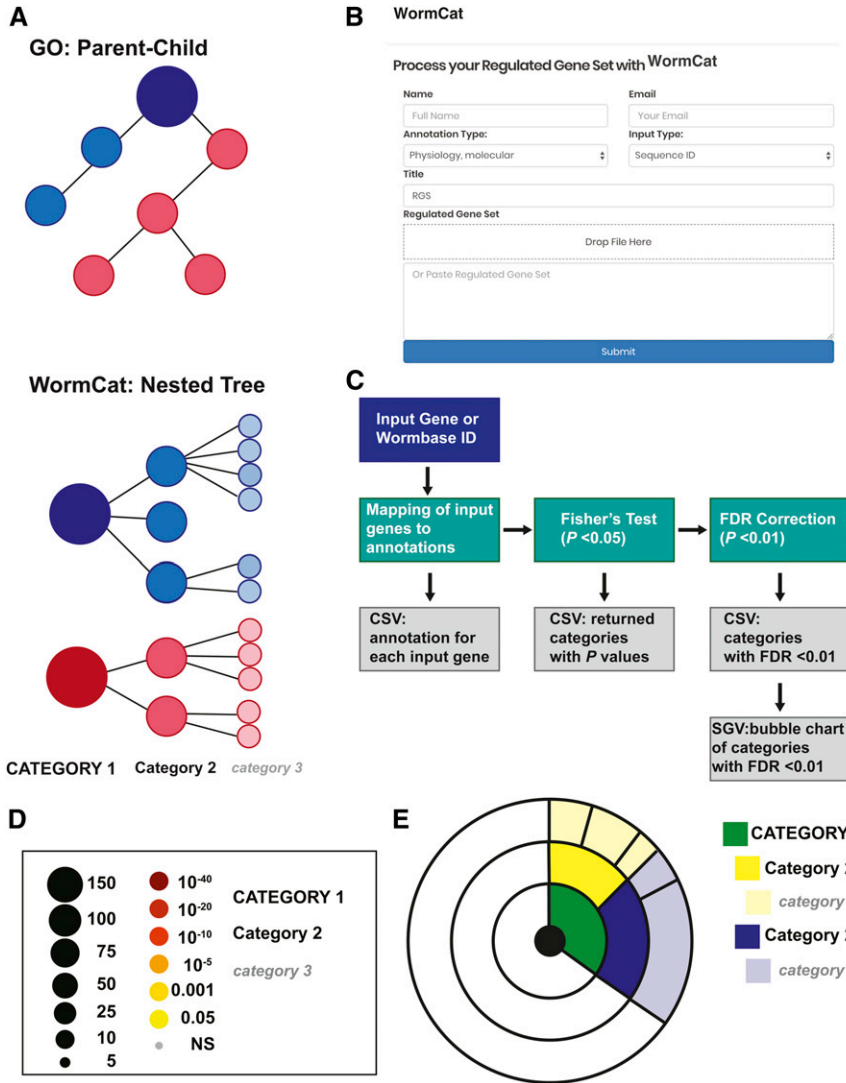


**Figure 1** WormCat annotates and visualizes *C. elegans* gene enrichment from genome-scale data. (A) Diagram comparing the parent-child methods for linking GO terms with the nested tree strategy used for annotating *C. elegans* genes in WormCat. (B) Screenshot of the WormCat web page showing the data entry form. (C) Flow chart diagramming steps and outputs from the WormCat program. Data outputs are in tabular comma-separated values (CSV) and scalable vector graphics (SVG) formats. (D) Legend for scaled bubble charts showing the number of genes referenced to size and  $P$ -value referenced to color. In graphs, Category 1, 2, and 3 are differentiated by capitalization, size, and italics. (E) Legend for sunburst plots showing concentric rings visualizing Category 1, 2, and 3 data.

the WormCat annotation list used as background so that the same background set was used when comparing WormCat and GOrilla. “All” was selected for ontogeny choices, and the  $P$ -value thresholds were set to  $10^{-3}$ . Output selections were Microsoft Excel and REVIGO (Supek *et al.* 2011).

## Results

### *C. elegans* gene annotation

The *C. elegans* genome encodes ~19,800 protein-coding genes, ~260 microRNAs, and numerous other noncoding RNAs (WormBase version WS270). We annotated all *C. elegans* genes first based on physiological functions, and, when these functions were unknown or pleiotropic, according to molecular function or subcellular location (see Supplemental Material, Table S1 for annotations, Table S2 for Category definitions). Our annotations are structured as nested categories, enabling classification into broad (Category 1; Cat1), or more specific categories (Category 2 or 3; Cat2 or Cat3). This annotation has the advantage of including information

from multiple sources in addition to GO. For example, we used phenotype information available in WormBase (Lee *et al.* 2018) for Cat1 assignments. Importantly, the phenotypic data present in WormBase (Lee *et al.* 2018) was used only if phenotypes were: (1) derived from wild type animals, (2) examined in detail in peer-reviewed publications, and (3) represented in two independent screens. If a gene was ascribed a clear physiological function with these criteria, we assigned it to a physiological category, examples of which include *Stress response*, *Development*, and *Neuronal function*. If gene products have multiple functions within the cell, act in multiple cells type, or different developmental times, we prioritized assignment to molecular categories. Molecular categories harbor both genes whose products comprise molecular machines, as well as the chaperones or regulatory factors that are necessary for the function of such machines. We used information on the molecular function of human orthologs to classify *C. elegans* genes that had not been molecularly defined in nematodes, and were highly similar in BLAST scores. For example, we classified the *C. elegans* gene W03D8.8 in *Metabolism: lipid: beta-oxidation* based on a

BLAST score of  $e = 7 \times 10^{-37}$  and similarity over 92% of its length to human ACOT4 (acyl-CoA thioesterase 4). For genes with weaker homology to human genes, we further refined assignments using BLAST (Altschul *et al.* 1990) and the NCBI Conserved Domain server (Marchler-Bauer *et al.* 2017). We used these tools to determine if there was significant homology or shared domains between *C. elegans* and human proteins, then used information in UniProt ([www.uniprot.org](http://www.uniprot.org)) for the human proteins to determine molecular classification. For example, we placed the *C. elegans* gene T26E4.3 in *Protein modification: carbohydrate*-based on a BLAST core of  $e = 4 \times 10^{-7}$  over 95% of its length to human alpha fucosyltransferase 1, and identification of a Fut1\_Fut2-like domain by the NCBI conserved domain server with an  $e$  score of  $6.16 \times 10^{-36}$ . However, while the gene BE10.3 is referred to in the WormBase description as an ortholog of human FUT9 (fucosyltransferase (9)) (Table S1), we found no homology to human genes by NCBI BLAST or domain conservation across all organisms with the NCBI Conserved Domain server. Therefore, we classified BE10.3 in *Unknown*. Finally, if no biological or molecular function could be assigned, protein subcellular localization was used for annotation. For example, a protein with a predicted membrane-spanning region that lacks characterization as a receptor would be placed in *Transmembrane protein*. Genes with no functional information were classified as *Unknown* (Cat1). A total of 8160 genes lacked sufficient information for classification in physiological, molecular, or subcellular localization categories, and were classified in *Unknown*. Many of these genes are *C. elegans*- or nematode-specific; however, some have homology to human genes of unknown function. WormBase also aggregates microarray and RNA-seq information, and annotates genes that respond to pharmacological treatments (Lee *et al.* 2018). We also used this information to differentiate genes within *Unknown: regulated by multiple stresses* that respond to at least two commonly used stressors. This classification does not imply that these genes have a function in the stress response. It does allow identification of genes with otherwise unknown functions that are common responders to stress. This classification may be useful to distinguish RNA-seq datasets that respond similarly to pharmacological stressors or can serve as a source to identify specific genes of interest for additional study. We also included pseudogenes and noncoding RNAs in our annotation list. These genes commonly appear in RNA-seq data; including them in the annotation list allows them to be labeled within the user's input dataset. In this way, we were able to leverage multiple data sources to categorize *C. elegans* genes into potentially functional biological groups.

#### **WormCat.com allows web-based searches of input genes and generates scaled bubble charts and gene lists**

WormCat.com maps annotations to input genes then determine category enrichment for Cat1, Cat2, and Cat3 (Figure 1B). Determination of category enrichment in a gene set of interest compared to the entire genome can rely on several

commonly used statistics such as the Fisher's exact test and the Mann-Whitney test (Mi *et al.* 2019). We used Fisher's exact test to determine if categories were over-represented because it is accurate down to small sample sizes, which may occur in high-resolution classifications (McDonald 2014). In addition, we included the Bonferroni FDR correction (McDonald 2014). To determine the number of false positives after Fisher's test or the FDR correction, we tested randomized gene lists of 100, 500, 1000, or 1500 genes and found that small numbers of genes were returned using a  $P$ -value cut-off of 0.05 (for, example 5 genes were returned on the 1000 gene random set). Few genes were returned from any of the randomized sets using an FDR cutoff of 0.01 (Table S3). Because an FDR  $< 0.01$  is relatively stringent, Fisher's exact test  $P$ -values will also be provided, allowing users to make independent evaluations on the statistical cut-offs.

The WormCat website ([www.wormcat.com](http://www.wormcat.com)) provides gene enrichment outputs in multiple formats (Figure 1C). First, all input genes are listed with mapped annotations (`rgs_and_categories.csv`). Genes that matched at least one Cat1, Cat2, and Cat3 classification are returned with Fisher's exact test  $P$ -values (`Cat1.csv`, `Cat2.csv`, or `Cat3.csv`). Next, Cat1, Cat2, and Cat3 matches with an FDR correction of  $< 0.01$  are returned as CSV files named `Cat1.apv`, `Cat2.apv`, and `Cat3.apv` (appropriate  $P$ -value). Finally, the `Cat.apv` files are used to generate two types of graphical output. First, it constructs scaled heat map bubble charts (`Cat1.`, `Cat2.`, `Cat3.sgv`) where color signifies  $P$ -value, and size specifies the number of genes in the category (Figure 1D). The scaling for these graphs is fixed so that multiple datasets can be graphed together. Second, a sunburst graph is built with concentric rings of Cat1, Cat2, and Cat3 values (Figure 1E). In these graphs, rings sections correspond to categories, with section sizes proportional to numbers of genes in the category. On the website, each ring section is clickable to generate a subgraph-based division within a section. For example, clicking a single Cat1 section would generate a subgraph with all the Cat2 and Cat3 subdivisions located within. This graphical output is likely to be most useful for visualization of a single RNA-seq dataset, or genetic screening data. Thus, WormCat provides multiple outputs to allow inspection of individual input genes, generation of gene tables, and  $P$ -values, and graphical visualization of enrichments.

#### **Comparison of GO and WormCat analysis of *sams-1*(RNAi) enrichment data**

To determine the utility of the WormCat annotations, we first analyzed microarray data we had previously generated to compare gene expression changes after knockdown of *sams-1*, with and without dietary supplementation of choline (Ding *et al.* 2015). *sams-1* encodes an S-adenosylmethionine (SAM) synthase, which is an enzyme that produces nearly all of the methyl groups used in methylation of histones and nucleic acids, in addition to the production of the membrane phospholipid phosphatidylcholine (PC) (Mato and Lu 2007).

*sams-1* RNAi or loss-of-function (*lof*) animals have extended lifespan (Hansen *et al.* 2005), increased lipid stores (Walker *et al.* 2011), and activated innate immune signatures (Ding *et al.* 2015). *sams-1* animals have low PC (Walker *et al.* 2011), but those levels are restored with supplementation of choline (Ding *et al.* 2015), which supports SAM-independent phosphatidylcholine synthesis (Vance 2014) (Figure 2A). Gene expression changes in *sams-1*(RNAi) animals could result from a perturbation in different SAM-dependent pathways. To determine which transcriptional changes occurred downstream of alterations in PC synthesis, we performed microarrays with RNA from *sams-1*(RNAi) and *sams-1*(RNAi) animals supplemented with choline; 90% of genes that changed in expression in *sams-1*(RNAi) animals returned to wild-type levels after choline supplementation. Therefore, the expression of the remaining 10% of genes was altered by *sams-1* RNAi independently of phosphatidylcholine levels (Ding *et al.* 2015).

In order to identify GO terms enrichment with WormCat, we submitted genes up- or downregulated twofold or more in *sams-1*(RNAi) animals to both WormCat and GOrilla (Eden *et al.* 2009). We used REVIGO (Supek *et al.* 2011) to visualize GO output. Both GOrilla/REVIGO (Figure 2B, Figure S2, A and B, and Table S4) and WormCat (Figure 2C and Table S5) identified categories of stress-response and metabolism linked to lipid accumulation in the genes that are upregulated upon *sams-1* RNAi, which is in agreement with our previous analysis (Ding *et al.* 2015). Interestingly, the relative importance of lipid metabolism is different in the two analyses. In the WormCat analysis, *Metabolism: lipid* was the third most enriched Cat2 category with a *P*-value of  $1.2 \times 10^{-9}$  (Table S5). In the GO analysis, however, *lipid metabolic process* was found with a modest enrichment of FDR corrected *P*-value =  $5 \times 10^{-2}$  (Table S4). WormCat identified 41 genes in the *Metabolism: lipid* category, whereas GOrilla's GO term search identified 33 genes in *lipid metabolic process* (Figure 2E and Table S4). Further inspection showed that six of the genes identified by solely by GOrilla were phospholipid lipases or phosphatases, one was an undefined hydrolase with no domain similarity to genes with known lipid functions, and one was a transmembrane protein. Each of these genes may be better classified in other categories (see Table S4 for GO lipid genes annotated by WormCat, tab 5 "GO\_lipid\_sams\_up"). For example, lipases that hydrolyze phospholipids are the endpoints of metabolic pathways but produce second messengers acting in signaling pathways. One of these genes, Y69A2AL.2, has significant similarity to the human phospholipase A2 gene, PLA2G1B (BLAST *e* score of  $2 \times 10^{-11}$ ). This class of phospholipases cleave 3-sn-phosphoglycerides to produce the signaling molecule arachidonic acid (Xu *et al.* 2009); therefore, a classification of *Signaling* is likely more reflective of its biological function than *Metabolism: lipid*. Taken together, WormCat identifies more genes that are directly relevant to the increased lipid storage phenotype observed with *sams-1*(RNAi) or (*lof*) animals (Walker *et al.* 2011; Smulan *et al.* 2016).

Next, we compared WormCat analysis of *sams-1*(RNAi) upregulated genes to the Gene Set Enrichment Analysis (GSEA) tool located in the WormBase suite (Angeles-Albores *et al.* 2016). GSEA, a GO-based tool, identified similar categories as GOrilla, with a concurrently high score for *the lipid catabolic process* (Figure S1). Our test set included 773 genes (Table S5, tab4); however, 286 of these genes were excluded from the GSEA analysis (Table S6), similar to the percentage excluded in a GOrilla analysis (Ding *et al.* 2018). Unlike GOrilla, GSEA provides the user with gene IDs of excluded genes (Table S6). Therefore, we asked if these genes were excluded because their functions were undefined, or if they were instead capable of classification. We found that 118 of the 286 excluded genes were classified as *Unknown* by WormCat (Table S6). However, 92 of the 476 genes GSEA included were also *Unknown* in WormCat analysis (Table S5, tab 4). Thus, genes within this set that are classified as *Unknown* by WormCat only partially overlap with genes excluded from GO analysis. Furthermore, WormCat classified 117 genes within the 286 genes excluded from GSEA, with 16 in noncoding categories and the remaining 101 in protein-coding categories such as *Cytoskeleton*, *Metabolism*, and *Proteolysis: proteasome* (Table S6). Thus, analysis of genes excluded from GO shows that an important fraction can be annotated and that *Unknown* WormCat categories are represented in both genes included and excluded from GO analysis.

Next, we used WormCat to analyze genes downregulated in *sams-1*(RNAi) animals. We noted enrichment in *Development: germline and mRNA function* categories in *sams-1*(RNAi) animals, and that this enrichment is lost with choline treatment (Figure S2D and Table S5). This is consistent with the reduction in embryo production after *sams-1*(RNAi), and the rescue of fertility when choline supplementation restores PC levels (Walker *et al.* 2011; Ding *et al.* 2015). *Stress response* categories, however, are enriched in downregulated genes from both *sams-1*(RNAi) and *sams-1*(RNAi) choline-treated animals (Figure S2C and Table S5). This appears to contrast with the complete loss of enrichment after choline treatment in the upregulated stress-response genes (Figure 2C and Table S5). However, an inspection of the annotated gene lists returned by WormCat shows that the individual genes within the downregulated *Stress response* category are different (Figure S2E and Table S5). Thus, on a gene by gene level, this data shows that the effects of choline supplementation are distinct for the up- and downregulated genes in the *Stress response* category. In addition, this demonstrates that, by providing both gene set enrichment and annotation of individual genes, WormCat provides a level of analysis that is difficult to achieve by traditional GO methods.

### ***Tau-tubulin kinases family are enriched in spermatogenic germlines***

*C. elegans* is a robust model system for studying development and differentiation. The study of hermaphrodite germline development has been of particular interest, as it first produces sperm, after which it switches to oocyte production

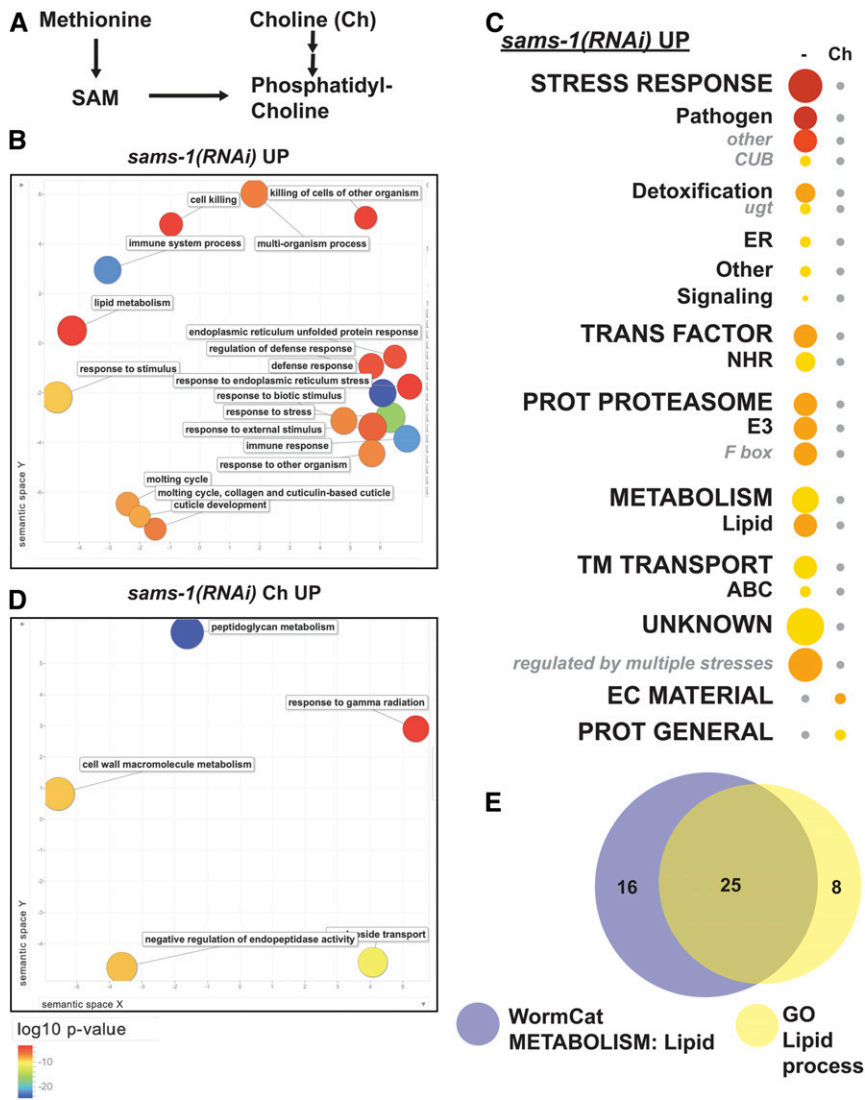


**Figure 2** WormCat verifies known category enrichments *sams-1(RNAi)* upregulated genes. (A) Schematic showing metabolic pathways linking methionine, SAM, choline, and phosphatidylcholine production. Gene expression microarray data for (B–D) were obtained from Ding *et al.* (2015). (B) Semantic plot of GO enriched classifications generated by REVIGO (Supek *et al.* 2011) from *sams-1(RNAi)* Up genes. (C) WormCat visualization of categories enriched in genes upregulated in *sams-1(RNAi)* animals with and without choline supplementation in order of Cat1 strongest enrichment. Categories 2 and 3 are listed under each Category 1, with Category 2 or 3 sets that appeared independently of a Category 1 listed last. Bubble heat plot key is the same as Figure 1D. (D) *sams-1(RNAi)* Up plus choline (Ch) genes visualized by REVIGO. (E) Venn diagram showing overlap between WormCat *Metabolism: lipid* and GO *Lipid process* gene annotations. ABC, ATP-Binding Cassette; Ch, Choline; CUB, Complement C1r/C1s, Uegf, Bmp1 domain; EC Material, Extracellular Material; NHR, Nuclear Hormone Receptor; Prot General, Proteolysis General; Prot Proteasome, Proteolysis Proteasome; SAM, S-adenosylmethionine; TM Transport, Transmembrane Transport; ugt, UDP-glycosyltransferase

(Hubbard and Greenstein 2005). This concurs with distinct gene expression programs for both processes (Greenstein 2005; Ehnault 2006). Recently, the Kimble laboratory performed RNA-seq on dissected germlines from genetically female [*fog-2(q71)*] and genetically male [*fem-3(q96)*] animals (Ortiz *et al.* 2014) (Figure 3A). Genes expressed in both germlines were called gender-neutral (GN), in contrast to genes that are specific to female (Oo, oogenic) or male (Sp, spermatogenic) germlines (Ortiz *et al.* 2014). We used WormCat to determine enrichment categories in each dataset. We found that GN genes are strongly enriched for growth, DNA, transcription, and mRNA functions (Figure 3B and Table S7), which is expected because the germline is undergoing extensive mitotic and meiotic divisions. We further found that *Chromosome dynamics* and *Meiotic functions* were enriched in the GN dataset (Figure 3C and Table S7), as were *mRNA functions* of *Processing* and *Binding* (Figure 3D and Table S7). Oo genes were enriched for mRNA binding proteins, especially the zinc finger (ZF) class (Figure 3D and Table S7). These include such as maternally

deposited *oma-1*, *pie-1*, *pos-1*, and *mex-1*, *mex-5*, and *mex-6* mRNAs, which are known to function in oocytes (Lee and Schedl 2006) (Table S7). ZF proteins with unknown nucleic acid binding specificity were also enriched in the Oo dataset (Figure 3D and Table S7), suggesting that many of these may also be produced in the maternal germline. In an independent dataset comparing RNA from germline-less [*glp-4(bn2)*], oocyte [*fem-3(gof)*] and sperm-producing [*fem-1(lof)*] animals by microarray analysis (Reinke *et al.* 2000), we also observed enrichment in categories for mRNA functions, transcription, development, and cell cycle control (Figure S3, A–D and Table S8).

As expected, Sp genes are enriched for *Major Sperm Proteins* (MSPs), which are necessary for sperm crawling (Figure 3B and Table S7). Interestingly, a class of potential cytoskeletal regulators, *tau-tubulin kinases* (TTKs), were also enriched in Sp genes (64 of 71, *P*-value of  $8.8 \times 10^{-34}$ ) (Figure 3E and Table S7). One TTK, *spe-6*, was previously isolated in a screen for spermatogenesis defects, and is thought to be involved in phosphorylation of MSPs to allow

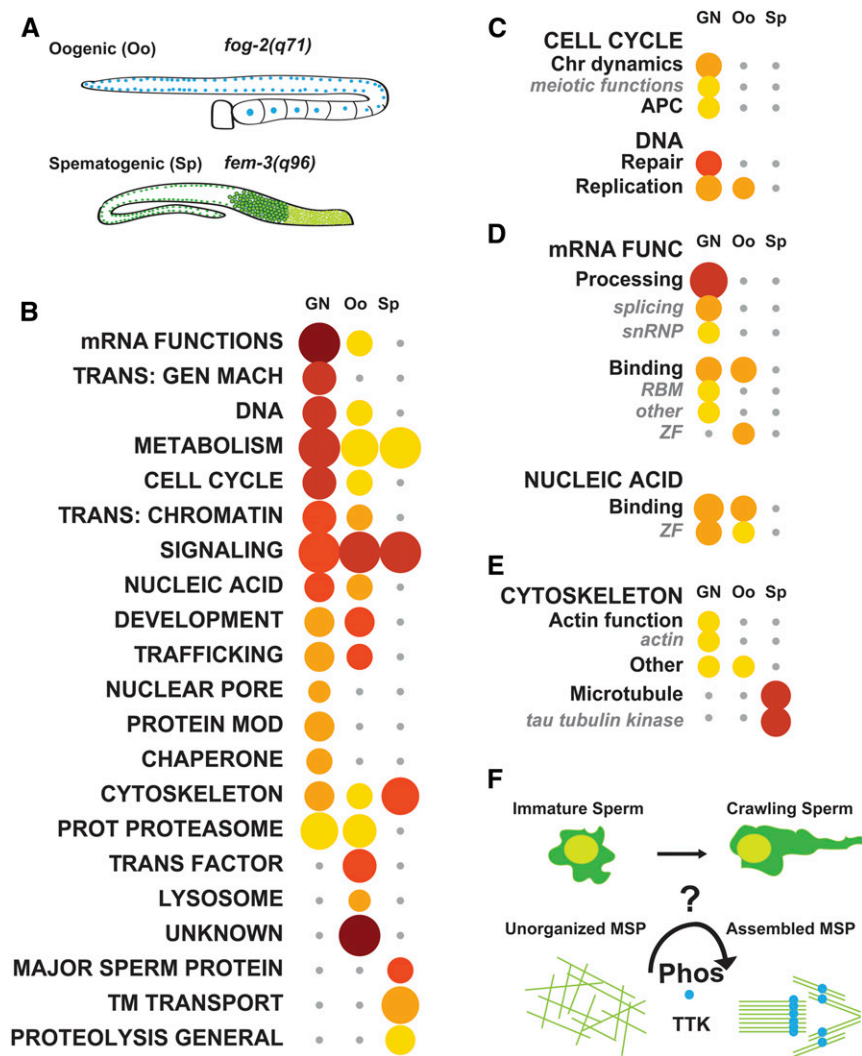


**Figure 3** Analysis of germline-specific RNA-seq data identifies the tau tubulin kinase family as a male-specific category. (A) Schematic showing germlines used for female (top) or male (bottom)-specific RNA-seq analysis from Ortiz *et al.* (2014) and the mutant alleles to cause these phenotypes. (B) WormCat Category 1 analysis of Germline neutral (GN), Oogenic (Oo), or Spermatogenic (Sp) datasets ordered by most enriched in GN data. (C–E) Breakdown of WormCat enrichment from the Category 1 level for Cell Cycle (C), mRNA Functions and Nucleic Acid (D), and Cytoskeleton (E). Bubble heat plot key is the same as Figure 1D. (F) Schematic showing predicted phosphorylation and organization of MSPs during *C. elegans* sperm maturation based on WormCat findings. APC, Anaphase Promoting Complex; Chr Dynamics, Chromosome Dynamics; mRNA Func., mRNA Function; MSP, Major Sperm Protein; Phos, Phosphorylation; Protein Mod, Protein Modification; Prot Proteasome, Proteolysis Proteasome; RBM, RNA Binding Motif; TTK, Tau Tubulin Kinase; TM Transport, Transmembrane Transport; Trans: Gen Mach, Trans: Chromatin, Transcription: Chromatin; Transcription: General Machinery; Trans Factor, Transcription Factor; ZF, Zinc Finger

the sperm to crawl (Varkey *et al.* 1993). Underscoring the potential importance of the TTKs in the male germline, WormCat also produced an enrichment in *tau tubulin kinases* in the Reinke *et al.* (2000) spermatogenic gene sets (Figure S3E and Table S8). Thus, WormCat has identified a class of kinases that may be important for sperm-specific functions (Figure 3F).

To directly compare gene set enrichment from WormCat and GO, we analyzed each of these germline-enriched datasets with GOrilla and used REVIGO (Supek *et al.* 2011) for visualization (Figure S4, A–C, Figure S5, A and B, Table S7, and Table S8). For the GN genes, the top 5 of the 544 significantly enriched categories were nucleic acid metabolic process (GO:0090304), nucleobase-containing compound metabolic process (GO:0006139), heterocycle metabolic process (GO:0046483), cellular aromatic compound metabolic process (GO:0006725), and organic cyclic compound metabolic process (GO:1901360) (Figure S4A and Table S7, see tabs 7, 8). These GO categories are highly overlapping and linked to multiple general processes involving nucleic acids. One gene GO:0006139, *gut-2*, an LSM RNA binding protein,

was present in 23 different GO categories (Table S7). A comparison of these GO categories found that each contains genes placed in distinct WormCat categories. For example, *gut-2* was placed in *mRNA Functions* in WormCat, *ama-1*, the RNA Pol II large subunit, placed in *Transcription: General Machinery*, *brc-1*, the BRCA1 ortholog, placed in *DNA* and *nsun-5*, a mitochondrial RNA methyltransferase placed in *Metabolism: mitochondria*. These WormCat categories are the top five identified in the GN dataset (Figure 3B and Table S7). Thus, while WormCat and GO are both identify nucleic acid-related processes as among the most highly enriched in the GN dataset, the WormCat data are more concise and easily aligned with the molecular processes.

Within the spermatogenic datasets from Ortiz *et al.* (2014) and Reinke *et al.* (2000), WormCat identified a class of kinases, tau tubulin kinases (TTKs), that have the potential to function in sperm motility. General categories of phosphorus metabolic process (GO:0006793), phosphate-containing compound metabolic process (GO:0006796), and peptidyl-threonine phosphorylation (GO:0018107) were among the top five most enriched categories by GO from the

Spermatogenic dataset; however, the TTKs as a group were not selectively identified from these very broad signaling categories in either spermatogenic data set (Table S7 and Table S8). Thus, WormCat provided advantages over GO in the germline data sets by providing less redundant, and more easily interpreted, data, and, most importantly, by identifying novel categories with potential links to biological function.

### **Identification of postembryonic tissue-specific gene expression categories**

Improved technologies for cell-type-specific marker expression, nematode disruption, and deep sequencing of small RNA quantities have allowed construction of gene expression datasets from larval (Spencer *et al.* 2011) and adult (Kaletsky *et al.* 2018) somatic tissues. To generate data from larval cell types, the Miller laboratory used cell-type-specific tagged green fluorescent proteins to label a wide variety of larval tissues, and examined mRNA expression in tiling microarrays (Spencer *et al.* 2011). RNA from each cell type would include tissue-specific, broadly expressed, and ubiquitously expressed genes. To define cell-type specific transcripts, Spencer *et al.* (2011) designated *selectively enriched genes* as expressed more than twofold vs. the whole animal and as present in a few cell types (Spencer *et al.* 2011). First, we performed WormCat analysis on the *selectively enriched* gene sets, and found distinct gene set enrichments for each tissue type (Figure 4A and Table S9). For instance, body wall muscle (BWM) was enriched for *Muscle Function* and *Cytoskeleton* (Figure 4B and Table S9). The category *Metabolism* was enriched in both intestine (Int) and hypodermis (Hyp), whereas *Stress responses* appeared more specific for the intestine, and *Extracellular material* for the hypodermis (Figure 4, B and C and Table S9). This likely reflects the role of the intestine in mediating contact with the bacterial diet, and the importance of the hypodermis for cuticle formation. While metabolic genes are expected to be required across multiple cell types, some cell types have specialized metabolic requirements. Lipid metabolism gene enrichment appeared at the Cat2 level in both intestine and hypodermis. However, Cat3 analysis shows that sterol and sphingolipid genes drive this enrichment in the intestine, while hypodermal lipid enrichment involves more broad categories, with minor enrichments in *Metabolism: lipid: binding* and *Metabolism: lipid: lipase* ( $P$ -values of  $4.51 \times 10^{-04}$  and  $2.86 \times 10^{-04}$ , which did not satisfy the FDR cutoff) (Figure 4D and Table S9). The Cat1 level analysis showed strong enrichment of transmembrane (TM) transporters in all tissues, including the intestine, excretory cells, and in neurons; however, the Cat2 level shows enrichment of distinct classes of transporters (Figure 4B and Table S9) aligning with functions such as nutrient uptake, waste processing, and channel activity in each of these cell types.

Next, we examined the data from Kaletsky *et al.* (2018), who performed RNA-seq from adult *C. elegans* sorted for muscle (Mus), intestinal (Int), hypodermal (Hyp), and neurons (Figure 4E and Table S10). They computationally

separated genes to distinguish expression specificity, demarking “enriched,” “unique,” and “ubiquitously” expressed categories. We used the “enriched” gene sets in WormCat analysis, and found that WormCat correctly mapped muscle or neuronal genes to those cell types (Figure 4F and Table S10). At the Cat1 level, *Extracellular material* was enriched in muscle, hypodermis, and intestine (Figure 4F and Table S10). At the Cat2 levels, *Extracellular material* diverged with *matrix* showing enrichment in muscle and *collagen*, showing enrichment in intestine and hypodermis (Figure 4G and Table S10). However, the collagen genes enriched in intestine and hypodermis were distinct (Figure 4G and Table S10), perhaps reflecting differing roles for these collagens in the cuticle vs. in basement membranes. Distinguishing individual genes for this comparison is very cumbersome in commonly used GO servers, and, therefore, represents an advantage of using WormCat. Previous studies found that two intestinal basement membrane collagens were produced in nonhypodermal tissues (Graham *et al.* 1997); however, this data suggests that the intestine others could produce others locally. Kaletsky *et al.* (2018) also noted enrichment of metabolic function in adult hypodermis with GO analysis. Metabolic gene enrichment was also detected by WormCat analysis of their data (Figure 4H and Table S10), as well as in the larval data from Spencer *et al.* (2011) (Figure 4D and Table S9).

In our annotation strategy, we chose to restrict genes in categories such as *Neuronal function* to those that are specific to that tissue, and that have a described physiological function. Genes that functioned in neurons, as well as other tissues, were placed in more general molecular function-based categories. With this approach, we hoped to reduce false-positive identification of neuronal categories outside the nervous system, yet permit the identification of related, yet functionally less-specific groups. For example, while the WormCat analysis of the neuronal tissues in the Spencer *et al.* (2011) and Kaletsky *et al.* (2018) datasets showed strong enrichment of neuronal-specific categories, it also included categories of genes likely to function in both neurons and other tissues, or that contained genes that had not yet been classified *in vivo*. These categories include *Metabolism: insulin* (Figure 4, D and H and Table S10), *Transmembrane (TM) transport*, *Signaling* (Figure 4, B and F and Table S10), and *Transmembrane protein* (Figure 4B and Table S10). This is in line with the analysis by both Kaletsky *et al.* (2018) and Ritter *et al.* (2013).

In order to distinguish the utility of WormCat from GO for the tissue-specific Spencer *et al.* (2011) and Kaletsky *et al.* (2018) datasets, we used GOrilla (Eden *et al.* 2009) to generate GO analysis, and visualized the data with REVIGO (Supek *et al.* 2011) (Figure S6, Figure S7, Figure S8, Table S9, and Table S10). There were many similarities between the categories. For example, categories linked to the *Cytoskeleton* are highly enriched in the muscle datasets from Kaletsky *et al.* (2018) by GOrilla and WormCat (Figure 4F, Figure S7A, and Table S10). In another example, *Stress response* categories were highly enriched by both WormCat and

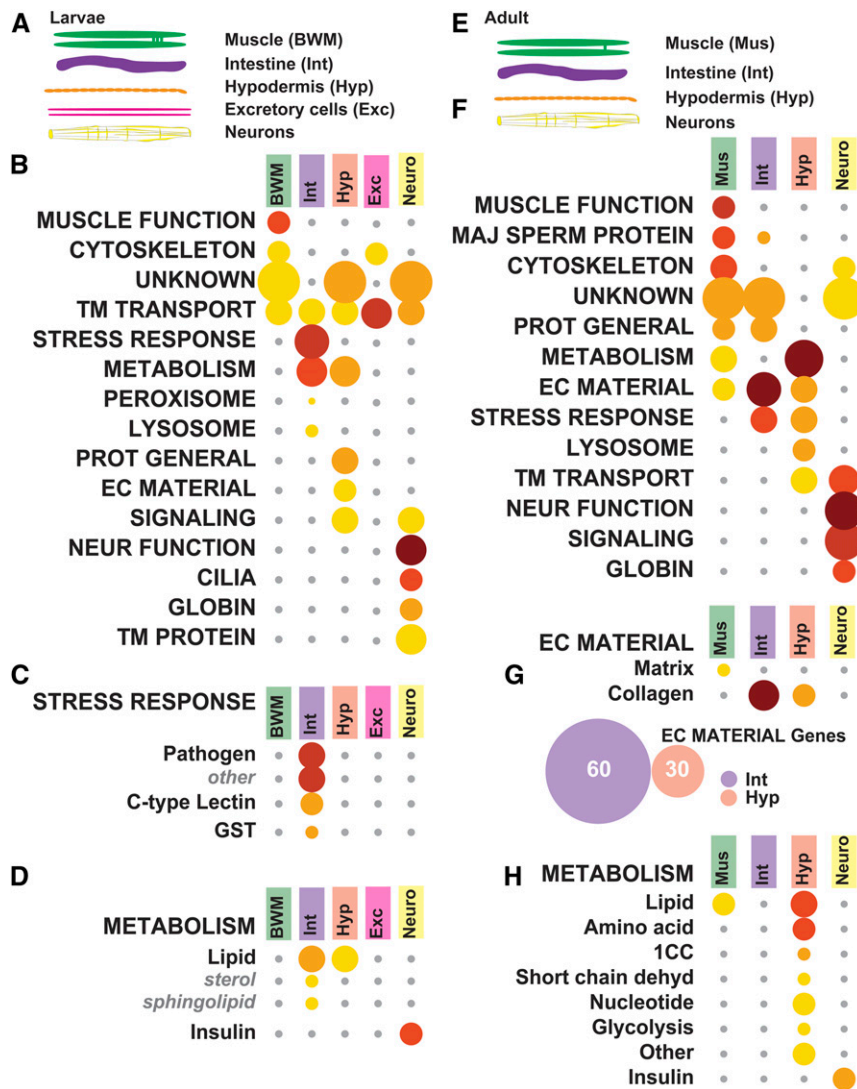


**Figure 4** WormCat analysis of tissue-specific gene sets reveals the importance of the intestine in stress-responsive categories. (A) Diagram showing larval tissues isolated in tiling array data used in figures B–D from Spencer *et al.* (2011) (B) WormCat Category 1 enrichment for larval tissue-specific *selective enriched* gene sets shows differentiation of Body wall muscle (BWM), Intestine (Int), Hypodermis (Hyp), Excretory cells (Exe), and Neurons. (C–D) Category 2 and 3 breakdown of Stress Response (C) and Metabolism (D). (E) Schematic showing adult tissues isolated for RNA-seq used in figures F–I from Kaletsky *et al.* (2018) (F) Category 1 analysis of enriched genes shows the differentiation of muscle and neuronal functions. (G–H) Category 2 and 3 breakdown of Extracellular Material gene enrichment, including a Venn diagram showing relationships between collagen genes in intestine and hypodermis (G), and Metabolism (H). Bubble heat plot key is the same as Figure 1D. 1CC, 1-Carbon Cycle; EC Material, Extracellular Material; GST, Glutathione-S-transferase; Maj Sperm Protein, Major Sperm Protein; Neur Function, Neuronal Function; Prot General, Proteolysis General; Short Chain Dehyd, Short Chain Dehydrogenase; TM Transport, Transmembrane Transport

GO in the larval (Spencer *et al.* 2011) and adult (Murphy *et al.* 2003) intestine (Figure 4F, Figure S6B, Figure S7B, and Table S10). However, as shown above, WormCat identified the insulin gene family as strongly enriched in both larval (Figure 4D) and adult (Figure 4H) neuronal tissue. Insulins were not identified as a class by our GO analysis. Instead, they were distributed among less specific categories such as biological regulation (GO:0065007), regulation of biological process (GO:0050789), and regulation of cellular process (GO:0050794) (Figure S5, Figure S6, Table S9, and Table S10). Thus, WormCat finds the major categories shown by GOrilla in the tissue-specific data, and also identifies additional enriched groups.

The seven transmembrane (7TM) protein family in *C. elegans* presented an annotation challenge. This class comprises ~8% of all protein-coding genes that seem likely to function in neurons, yet whose functions are undescribed (Robertson and Thomas 2006). Some have significant homology to mammalian G protein-coupled receptors (GPCRs), while others are nematode or *C. elegans* specific (Robertson and Thomas

2006). In order to identify and classify these proteins as accurately as possible, GPCRs with strong evidence for neuron-specific activity were placed in *Neuronal function*, while all other potential GPCRs were classified by protein domain and homology. For developing a list of potential GPCRs, we selected genes identified in WormBase as containing a transmembrane domain as well as those we initially annotated as GPCRs in the *Signaling* category. To recover any genes missed by these approaches, we added all *Unknown* proteins from our annotation list. We submitted the protein sequences for these genes to the NCBI Conserved Domain search tool (Marchler-Bauer *et al.* 2017), and selected all the genes in these groups that contained a 7TM domain (Figure 5A). Next, we used BLASTP to determine the degree of homology to human GPCRs, which would reflect the conservation of function. Genes that had BLASTP scores of  $e < 0.05$  on the NCBI server were classified in *Signaling: heteromeric G protein: receptor*. Those with  $e$  scores  $> 0.05$  were classified as *TM protein: 7TM*, with class designated by WormBase in Cat3. Thus, genes classified within *Neuronal function* or *Signaling*

have a strong likelihood of GPCR function, whereas those in *TM protein: 7TM* have not been sufficiently defined. *Signaling: G protein* categories are enriched in neuronal genes sets from both Kaletsky *et al.* (2018) and Spencer *et al.* (2011) (Figure 5, B and C, Table S9, and Table S10), and 7TM proteins show enrichment in the larval pan-neuronal, *glr-1*-expressing neurons, and motor neurons (Figure 5C, Table S9, and Table S10). Thus, our annotation strategy allows separation of GPCRs with a high likelihood of neuronal function, yet still permits enrichment of the larger class of 7TM proteins in neuronal tissues.

In order to directly compare WormCat and GO on the larval neuronal data sets, we examined category enrichment of Spencer *et al.* (2011) pan-neuronal and motor neuron genes in GO by GOrilla (Eden *et al.* 2009), using REVIGO (Supek *et al.* 2011) for visualization (Figure S6, Figure S8, and Table S9). The most enriched category in the pan-neuronal or motor neuron datasets was G protein-coupled receptor signaling (GO:0007186). Next, we used WormCat to determine how we had annotated genes within GO:0007186, and found that this GO category included genes we had classified in *Signaling: Heteromeric G protein (G-alpha subunits and receptors)*, *Neuronal Function: Synaptic function* (neuropeptides and neurotransmitter receptors), and *TM protein: 7TM receptor* (Figure 5C and Table S9). While inclusion of the G protein signaling apparatus and neuropeptide ligands is appropriate for the broad category of G protein signaling, the GO categories do not differentiate between GPCRs with a high likelihood of function from the poorly classified 7TM proteins. In addition, many of the *nlp* genes listed in GO:0007186 are functionally uncharacterized, and, thus, it is not clear if they are *bona fide* GPCR ligands or could interact with other receptors outside of GPCR signaling (Li and Kim 2008). Therefore, WormCat improves on GO analysis for these datasets by providing more nuanced information on the function of these genes in GPCR pathways.

Neuronal genes from adult (Kaletsky *et al.* 2018) and larval (Spencer *et al.* 2011) gene sets also showed strong enrichment in Cat2 and Cat3 classifications within *Neuronal function*, such as *Synaptic function*, *neuropeptide*, and *neurotransmitter (nt) receptor* (Figure 5, D and E, Table S9, and Table S10). *Cilia* gene enrichment was also apparent in the pan-neuronal and dopaminergic larval gene sets (Figure 5D and Table S9). Neurons are the only ciliated cells in *C. elegans*, and cilia occur on multiple neuronal subtypes (Inglis *et al.* 2007). However, all dopaminergic neurons are ciliated (Inglis *et al.* 2007), and, are, therefore, more likely to show enrichment. Taken together, our WormCat analysis of these large tissue-specific gene sets provides a detailed view of gene classes specific to muscle, hypodermis, intestine, and neurons in larvae and adults. We have identified differential enrichment in lipid metabolism genes, and collagens from intestine and hypodermis defined a classification system for GPCRs and 7TMs, and identified *Cilia* as a major enriched category in dopaminergic neurons. Much of this information goes beyond what GO analysis reveals, and provides

predictions that can be useful to design future studies. Identification of these types of nuanced tissue-specific patterns is an important step to understanding how specific cell types function.

### **Drug interactions limiting lifespan induce changes in sterol metabolism**

*C. elegans* is particularly suited to studies determining gene expression changes in response to a panel of treatments in a whole animal, and to correlate these changes to physiological function. For example, Admasu *et al.* (2018) generated a complex gene expression dataset by performing parallel RNA-seq on animals treated with five lifespan-increasing drugs that affect distinct pathways (Allantoin, Rapamycin, Metformin, Psora-5, and Rifampicin). They used five pairwise combinations and three triple-drug combinations to determine if any combination lead to further lifespan extension, and to identify gene expression profiles associated with increased longevity (Admasu *et al.* 2018). They found that one triple-drug combination (Rifa/Psora/Allan) activated lipogenic metabolism through the transcription factor *SBP-1/SREBP-1*, and determined that the drug-induced longevity was dependent on *SBP-1* function (Admasu *et al.* 2018). The authors also made the striking observation that a distinct triple-drug combination (Rifa/Rapa/Psora) reduced lifespan, even though each single drug or drug pairs increased longevity (Admasu *et al.* 2018). To determine if any gene expression categories might explain this effect, we used WormCat to analyze category enrichment for the up and downregulated genes for each single drug, pairwise, or triple-drug combination (Figure 6A, Figure S9, Figure S10, Table S11, and Table S12). Similar to the author's KEGG analysis (Admasu *et al.* 2018), we observed *Metabolism: lipid* enrichment in long-lived Rifa/Rapa/Psora-treated animals (Figure 6A and Table S11); however, we also noted that *Metabolism: lipid* was enriched in all three combinations with WormCat. Next, we examined the up and downregulated genes to determine if any categories correlated with the failure to survive in the Rifa/Rapa/Psora treated animals. We did not find category signatures in the downregulated genes that appeared to correlate with the decrease in longevity (Figure S10 and Table S12). However, upregulated genes from the short-lived Rifa/Rapa/Psora treated animals were enriched in another specific class of lipid metabolic genes: sterol metabolism (Figure 6A and Figure S9). Closer examination of the single and pairwise combinations showed that the enrichment of sterol metabolic genes only appeared in the triple combination with poor survival (Figure 6B). *C. elegans* does not use cholesterol as a membrane component (Ashrafi 2007). Thus, this category does not include cholesterol synthesis genes, but does include genes involved in modification of sterols, for example, in steroid hormone production (Watts and Ristow 2017). Examination of individual genes (Table S11, Tab 18 Sterol Genes) showed that 5 of the 19 had lifespan phenotypes, and 4 had lethality related phenotypes in WormBase, consistent with their effects on survival in Admasu *et al.* (2018).

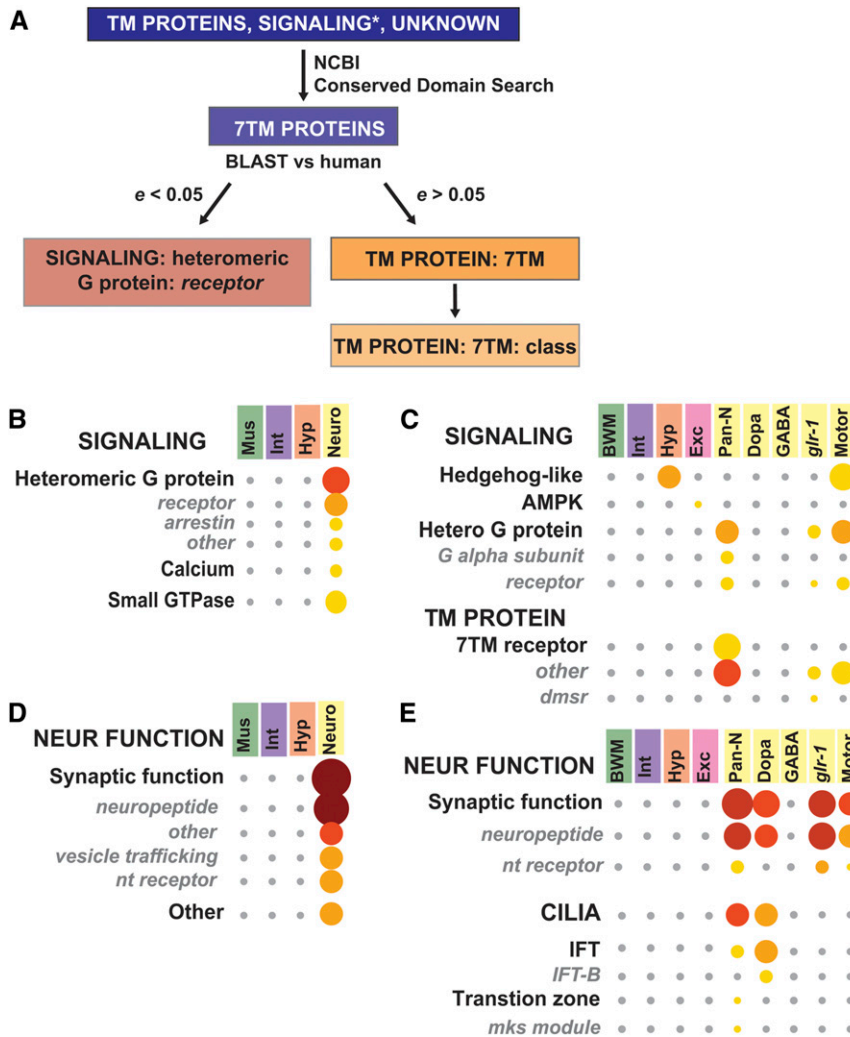


**Figure 5** Detailed analysis of neuronal tissue-specific gene sets reveals specific enrichment for cilia gene expression on dopaminergic neurons. (A) Flow chart showing the process for annotating seven transmembrane (7TM) proteins.  $e$  value is the statistical score provided by the NCBI BLAST server. Asterisk on Signaling notes that only predicted GPCRs within this category were submitted to the NCBI conserved domain server. (B–E) Breakdown of Neuronal Function to Category 2 and 3 from larval data in Kaletsky *et al.* (2018) (B and D) or adult data in Spencer *et al.* (2011) (C and E). 7TM receptor, Seven Transmembrane Receptor; BWM, Body Wall Muscle; dmsr, DroMyoSuppressin Receptor Related; Dopa, Dopaminergic Neurons; Exc, Excretory Cells; GABA, Gamma-Aminobutyric Acid-Specific Neurons; *glr-1*, Glutamate Receptor-Specific Neurons; Hetero G protein, Heterotrimeric G Protein; Hyp, Hypodermis; IFT, Intraflagellar Transport; Int, Intestine; mks module, Meckel-Gruber syndrome Module; Motor, Motor Neurons; nt Receptor, Neurotransmitter Receptor; Neuro, Neurons; Pan-N, Pan-Neuronal

Furthermore, Murphy *et al.* (2003) showed that 3 of the 19 sterol genes are upregulated in another long-lived model, *daf-2(mu150)*, and two of these, *stdh-1* and *stdh-3* are required for lifespan extension in *daf-2(mu150)* animals (Murphy *et al.* 2003). Thus, the category enrichments captured by WormCat for this drug study have identified sterol metabolism genes as potential players in the paradoxical lifespan shortening effects of the Rifa/Rapa/Psora combination.

In order to compare gene set enrichment of the triple-drug combinations from WormCat with GO, we analyzed upregulated genes from the Rifa/Psora/Allan-, Rifa/Rapa/Allan-, and Rifa/Rapa/Psora-treated animals in GOrilla (Eden *et al.* 2009), and visualized the data with REVIGO (Supek *et al.* 2011) (Figure S11 and Table S11). WormCat and GO showed multiple similarities. For example, WormCat and GO identified extracellular matrix-linked categories in all three triple combinations (WormCat: EC MATERIAL; GOrilla: GO:0030198: extracellular matrix organization) (Figure S9 and Table S11). However, WormCat identified *Metabolism: lipid* in all three combinations, whereas GO analysis by GOrilla only identified categories linked to lipid metabolism (GO:0006629: lipid metabolic process

( $q = 5.63 \times 10^{-03}$ ), GO:0044255 cellular lipid metabolic process ( $q = 1.49 \times 10^{-02}$ ) and GO:0006631 fatty acid metabolic process ( $q = 2.16 \times 10^{-02}$ ) in the Rifa/Rapa/Psora dataset (Table S11). WormCat also showed a much higher enrichment score for *Metabolism: lipid*,  $P = 2.00 \times 10^{-14}$ ) (Table S11). Thus, as in the *sams-1* microarray data discussed previously, WormCat provides an improved tool for determining the enrichment of metabolic genes.

WormCat also found an enrichment of transcription factors in each of the triple combinations, with specific enrichments in nuclear hormone receptors and homeodomain genes in the Rifa/Psora/Allan-upregulated set (Figure S9) Enrichments of nuclear hormone receptors in *C. elegans* is potentially of interest as they may regulate multiple metabolic regulatory networks (Arda *et al.* 2010). However, GOrilla only identified categories linked to transcription factors (GO:0006355: regulation of transcription, DNA-templated, GO:0051252: regulation of RNA metabolic process, GO:2001141: regulation of RNA biosynthetic process, GO:1903506 regulation of nucleic acid-templated transcription, and GO:0019219 regulation of nucleobase-containing compound metabolic process) in the Rifa/Psora/Allan dataset. No individual class of

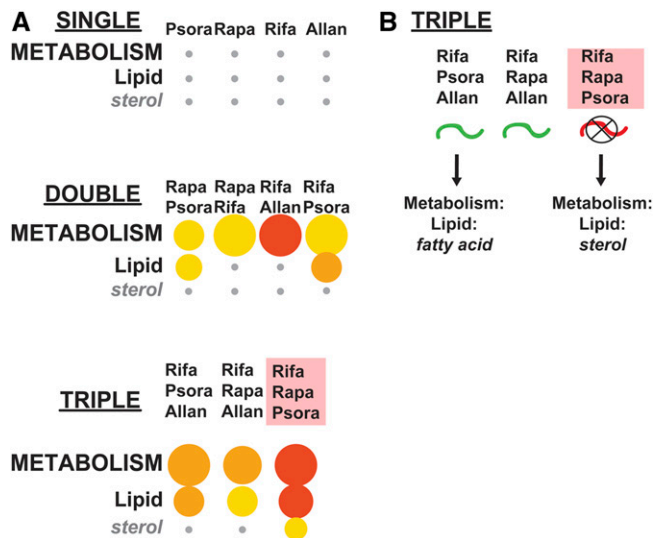


**Figure 6** WormCat analysis of RNA-seq data from *C. elegans* treated with combinations of lifespan-lengthening drugs reveals the emergence of sterol metabolism in drug combinations, limiting survival. (A) Comparison of *Metabolism: lipid: sterol* enrichment in single, double, and triple-drug combinations shows sterol emergence in the Rifa/Rapa/Psora gene set (Admasu *et al.* 2018). (B) Diagram showing a summary of data from lifespan changes after triple-drug treatment from Admasu *et al.* (2018). Pink box denotes drug combination that causes premature death. Bubble heat plot key is the same as Figure 1D. Allan, Allantoin; Psora, Psora-4; Rapa, Rapamycin; Rifa, Rifampicin

transcription factors showed enrichment in any of the triple combinations by GO (Table S11); thus, WormCat offers a clear advantage over GO by providing increased coverage across diverse categories of gene function.

#### Identification of gene set enrichments in RNAi screening data

In order to use WormCat to analyze genome-scale RNAi screening data, we mapped WormCat annotations to the list of genes in the Ahringer library (Kamath *et al.* 2003) (Table S13). To test this approach, we used data from the Roth laboratory, who screened the Ahringer library for changes in glycogen storage in *C. elegans* and identified >600 genes, scored as glycogen high, glycogen low, and abnormal localization (LaMacchia *et al.* 2015) (Figure 7A and Table S14). The authors functionally classified all hits from the screen with an inhouse annotation list, graphed the percentage within each group, and noted high percentages of genes with roles in metabolism (electron transport chain), signaling, protein synthesis or stability, and trafficking (LaMacchia *et al.* 2015); however, they were unable to assign statistical significance to any of the groups. WormCat identified similar groups as the LaMacchia *et al.* (2015) functional classification for the “glycogen low” candidates. For example, we identified *Metabolism: mitochondria*, complex I, III, IV, and V and found statistical enrichment in these categories (Figure 7B and Table S14). However, signaling had no enrichment (Table S14). Thus, WormCat can identify statistically relevant pathways in genome-scale RNAi screen data.

To provide a direct comparison between WormCat and GO with this dataset, we determined the GO term associated with the “glycogen low” data by GOrilla (Eden *et al.* 2009), and visualized the data with REVIGO (Supek *et al.* 2011) (Figure S12 and Table S14). A total of 185 separate GO terms were identified in this data set compared to the 4 Cat1 level terms identified by WormCat (*Metabolism*, *Lysosome*, *Proteolysis Proteasome*, and *Trafficking*) (Figure 7B and Table S14). WormCat also finds a limited number of Cat2 groupings within these sets, including *Metabolism: mitochondria*, *Lysosome: vacuolar ATPase*, *Proteolysis Proteasome:19S, 20S*, and *Trafficking: ER/Golgi* (Figure 7B and Table S14). This large difference in the number of significantly enriched categories stems from the multiple, overlapping categories present in the GO analysis. For example, the mitochondrial gene *cyc-1* (cytochrome *c* oxidase) is represented in 87 of the GO terms, whereas the annotation in WormCat is *METABOLISM: mitochondria* (Table S14, tab 8).

Similarly, the vacuolar ATPase *vha-6* appears in 39 of GO terms returned, the proteasomal component *pbs-7* is present in 23, and the ER/Golgi COP I component *Y71F9AL.17* is in 21 (see Table S14, tabs 9–11). This GO term redundancy provides the user with a complex, hard to interpret, list. In addition, GO terms that are repeated fewer times (such as those containing the trafficking gene *Y71F9AL.17*) become marginalized in a complex list. Thus, with this dataset, WormCat provides easily distinguished categories with clear links to biological or molecular functions. The GO terms show the same genes repeated in a large fraction of the categories and obscure categories with less gene redundancy.

## Discussion

### WormCat provides new insights into comparative RNA-seq data

Current technology allows for the routine use of genome-scale experiments for the generation of gene expression data. The goal of these experiments is often to identify classes of genes that add insight to biological functions, as well as to highlight selected genes for individual analysis. GO analysis, while widely used, is difficult to apply to datasets with multiple combinations of treatments or genetic perturbations. Further, for *C. elegans*, current GO analysis is often inaccurate, and misses useful physiological and molecular information. Here, we have shown that WormCat can annotate gene categories, provide enrichment statistics, and display user-friendly graphics for gene sets identified from *C. elegans* gene expression studies. Furthermore, our visualization strategy allows comparison across multiple datasets, facilitating the identification of categories with shared biological functions.

Our initial, script-based, smaller-scale version of WormCat highlighted changes in metabolic gene expression in *C. elegans* with changes in levels of the methyl donor SAM or methyltransferases modifying H3K4me3 (Ding *et al.* 2018). In this study, we have expanded the annotation list,

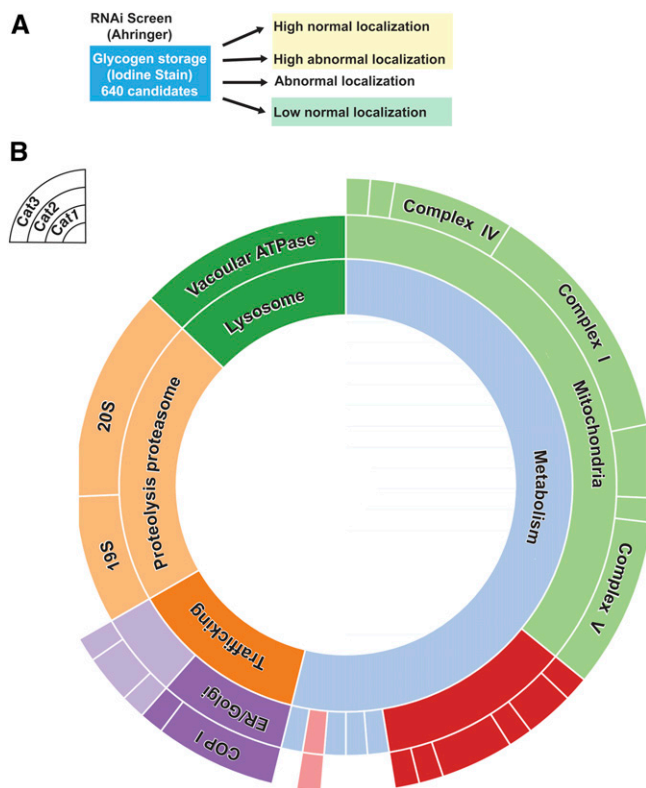


**Figure 7** WormCat analysis of a genome-scale RNAi screen quantitates categories of candidate genes. (A) Schematic of the RNAi screen from LaMacchia *et al.* (2015) identifying candidate genes that altered glycogen staining. (B) Sunburst diagram from low glycogen candidates showing significantly enriched categories.

developed a web-based server, and added a new graphical output. We used WormCat to successfully analyze data from metabolic, tissue-specific, and drug-induced expression changes. This analysis provides not only validation and use-case examples, but also additional insights into the known gene expression patterns. For example, our examination of germline gene expression datasets from the Kimble and Kim laboratories (Reinke *et al.* 2000; Ortiz *et al.* 2014) identified a large class of microtubule kinases (TTK) as enriched in spermatogenic gene sets, and as a coenriched gene set with MSPs. One TTK, *spe-6*, has been previously identified in a screen for mutants with defects in sperm development (Varkey *et al.* 1993). Our results suggest that many genes in this family could have important functions in spermatogenesis, and that the appearance of MSPs and TTKs in a dataset could also serve as a marker for maleness. Finally, we used WormCat to analyze a dataset consisting of RNA-seq from *C. elegans* treated with multiple lifespan-changing drugs, alone or in combination, plus one mutation animal strain that extends lifespan (Admasu *et al.* 2018). The classification and graphical output allowed us to identify the upregulation of sterol metabolism genes in a triple-drug combination that was not present in the single or double drug treatments. Thus, WormCat identified a gene set that may be important for the effects of the lifespan-altering drugs in this assay.

### Strengths and weaknesses of WormCat

We developed WormCat to overcome some of the limitations of GO analysis when analyzing *C. elegans* gene expression data, and to utilize specific phenotype data available in WormBase. In addition, we specifically engineered WormCat to classify data for the identification of coexpressed or cofunctioning gene sets. Finally, we developed two graphical outputs: a scaled heat map/bubble plot and a sunburst plot. The modular nature of the bubble plot allows multiple datasets to be grouped and compared, while the sunburst plot gives a concise view of single datasets, as may be obtained with screening data. Our validation with random gene testing and analysis of *C. elegans* gene expression data from metabolic, tissue-specific, and drug-treated animals shows that WormCat is a robust tool that provides biologically relevant gene enrichment information. There are three main areas that WormCat provides an advantage over using GO that are apparent in our case studies. First, as discussed above, we found that, in some of our test cases, WormCat identified broader sets of genes within categories or categories that were not identified by GO. Second, the WormCat output is much easier to interpret; the bubble charts provide intuitive visualization, and the tables provide clear access to the enrichment statistics and annotation of the input genes. Third, the availability of the annotations for each input gene enables comparisons between genes in categories. For example, we found that while *Extracellular material: collagen* was enriched in both intestine and hypoderm in the Kaletsky *et al.* (2018) data set, the genes were nonoverlapping, suggesting tissue-specific expression of collagen genes. This comparison would be difficult to make with GO, as many common GO servers do not supply the genes with each category in an easily accessible manner. Directly comparing the genes within WormCat and GO categories from our previously published dataset of gene expression after *sams-1* knockdown, we found that WormCat identified a broader set of lipid metabolic genes than GO analysis from GOrilla, and that the genes identified only by GO analysis might be better classified in different categories to reflect their biological functions. Thus, WormCat provides an alternative to GO with advantages in output that improve data interpretation and access to gene annotations that allow deeper comparisons among categories. In some cases, WormCat also identifies categories that are not found by GO.

However, there are several limitations to WormCat. First, while multiple researchers with varied expertise curated our annotation list, some genes may be misannotated, or some Cat2 or Cat3 groups may fit better in other Cat1 classifications. We will update the WormCat annotation list at periodic intervals while providing access to the previous annotation lists. Second, each *C. elegans* gene received a single, nested, annotation, rather than a group of annotations as in GO. We chose to prioritize the visualization of enriched gene sets in this instance, using a single annotation per gene to permit graphing in scaled heat maps. Access to the program and

annotation lists for the local application also allows users to customize the annotation lists according to their preferences.

Annotation lists of genome-scale data are likely to contain errors. We have defined several sources of error, and have taken corrective steps. In some cases, a gene may be simply misannotated. For example, a component of the *General transcription machinery* was placed in *Signaling* by the annotator. In others, the classification system may be incorrect. An example of this would be classifying enzymes that modify small molecules as protein modification. To estimate the misclassification error rate, we generated a list of 3000 random WormBase IDs. We mapped each ID to our annotation list and rechecked the annotations. We found 29/2294 genes (1.3%) whose annotations were incorrect by our criteria (13 of these were *Unknown* genes that could be classified in other categories). This suggests ~300 genes in the entire dataset may be misannotated by our criteria, many representing *Unknown* genes that could acquire classification. We will periodically update the WormCat annotation lists to accommodate new gene information and correct errors.

It is important to note that some gene classifications depend on criteria that are open to interpretation. For example, transcription factors regulating genes within a pathway are grouped within a linked category to allow identification of cofunctioning genes. For instance, *efl-1*, a master regulator of cell cycle genes, is annotated as *Cell cycle: transcriptional regulator*, instead of with the more broadly acting *trans-regulatory factors in Transcription factor: E2F*. To allow for different interpretations of the annotation strategy, we have set up a GitHub site (<https://github.com/dphiggs01/wormcat>), where the annotation list and scripts for executing WormCat can be downloaded and customized by the user to accommodate differences in annotation preference.

The value of gene set enrichment is also highly dependent on the criteria used to specify the regulated genes. In the present study, we used the same criteria as the respective authors, except that we separated up and downregulated genes where necessary. For example, in the Kaletsky *et al.* (2018) tissue-specific data, the authors provided data for all genes expressed in each tissue, enriched genes (expressed at FDR >0.05, and log<sub>2</sub> fold change >2 relative to other tissues), or unique genes (log<sub>2</sub> RPKM >5) significantly differentially expressed in comparison to the expression of each of the three other tissues (FDR >0.05, log<sub>2</sub> fold change >2 for each comparison) (Kaletsky *et al.* 2018). We found the best resolution of WormCat categories between the tissues occurred with the enriched datasets, rather than with all genes or unique gene sets. This suggests that gene lists with all expressed genes may require more stringent statistical cutoffs, but also that WormCat may not be as suited to highly filtered data.

### Application to other organisms

By developing WormCat specifically for analyzing *C. elegans* gene sets, we were able to take advantage of available data on WormBase, but this limited the applicability of our

annotation list with other organisms. Although researchers in mammalian fields can access pathway analysis pipelines such as Ingenuity Pathway Analysis (Qiagen; Krämer *et al.* 2014) that identify functionally linked genes, these programs do not necessarily provide a simple graphical output for comparative analysis. WormCat analysis generating the scaled heat/bubble charts can be adapted for use with other organisms by running the program locally with altered annotation lists. Replacing gene IDs and the Cat1, Cat2, and Cat3 values with any annotation allows customization of the pipeline to any other organism. Thus, the modular nature of WormCat allows adaptation to multiple annotation strategies within *C. elegans* or to other organisms, allowing a streamlined visualization for examining genome-scale expression or screen data.

### Acknowledgments

We wish to thank members of the Walker and Walhout laboratories for helpful discussion. Funding to A.K.W. National Institutes of Health (NIH) National Institute on Aging (NIA) 1R01AG053355 and A.J.M.W. grants NIH grants DK068429 and GM122502.

### Literature Cited

- Admasu, T. D., K. Chaithanya Batchu, D. Barardo, L. F. Ng, V. Y. M. Lam *et al.*, 2018 Drug synergy slows aging and improves healthspan through IGF and SREBP lipid signaling. *Dev. Cell* 47: 67–79.e5. <https://doi.org/10.1016/j.devcel.2018.09.001>
- Altschul, S. F., W. Gish, W. Miller, E. W. Myers, and D. J. Lipman, 1990 Basic local alignment search tool. *J. Mol. Biol.* 215: 403–410. [https://doi.org/10.1016/S0022-2836\(05\)80360-2](https://doi.org/10.1016/S0022-2836(05)80360-2)
- Angeles-Albores, D., R. Y. N Lee, J. Chan, and P. W. Sternberg, 2016 Tissue enrichment analysis for *C. elegans* genomics. *BMC Bioinformatics* 17: 366. <https://doi.org/10.1186/s12859-016-1229-9>
- Arda, H. E., S. Taubert, L. T. MacNeil, C. C. Conine, B. Tsuda *et al.*, 2010 Functional modularity of nuclear hormone receptors in a *Caenorhabditis elegans* metabolic gene regulatory network. *Mol. Syst. Biol.* 6: 367. <https://doi.org/10.1038/msb.2010.23>
- Ashburner, M., C. A. Ball, J. A. Blake, D. Botstein, H. Butler *et al.*, 2000 Gene ontology: tool for the unification of biology. The Gene Ontology Consortium. *Nat. Genet.* 25: 25–29. <https://doi.org/10.1038/75556>
- Ashrafi, K., 2007 Obesity and the regulation of fat metabolism (March 9, 2007), WormBook, ed. The *C. elegans* Research Community, WormBook, doi/10.1895/wormbook.1.130.1, <http://www.wormbook.org>.
- Baugh, L. R., J. Demodena, and P. W. Sternberg, 2009 RNA Pol II accumulates at promoters of growth genes during developmental arrest. *Science* 324: 92–94. <https://doi.org/10.1126/science.1169628>
- Bulcha, J. T., G. E. Giese, M. Z. Ali, Y. U. Lee, M. D. Walker *et al.*, 2019 A persistence detector for metabolic network rewiring in an animal. *Cell Rep.* 26: 460–468.e4. <https://doi.org/10.1016/j.celrep.2018.12.064>
- C. elegans Sequencing Consortium, 1998 Genome sequence of the nematode *C. elegans*: a platform for investigating biology. *Science* 282: 2012–2018 [corrigenda: *Science* 283: 35 (1999)]; [corrigenda: *Science* 283: 2103 (1999)]; [corrigenda: *Science* 285: 1493 (1999)].

- Deng, X., J. B. Hiatt, D. K. Nguyen, S. Ercan, D. Sturgill *et al.*, 2011 Evidence for compensatory upregulation of expressed X-linked genes in mammals, *Caenorhabditis elegans*, and *Drosophila melanogaster*. *Nat. Genet.* 43: 1179–1185. <https://doi.org/10.1038/ng.948>
- Ding, W., L. J. Smulan, N. S. Hou, S. Taubert, J. L. Watts *et al.*, 2015 S-adenosylmethionine levels govern innate immunity through distinct methylation-dependent pathways. *Cell Metab.* 22: 633–645. <https://doi.org/10.1016/j.cmet.2015.07.013>
- Ding, W., D. P. Higgins, D. K. Yadav, A. A. Godbole, R. Pukkila-Worley *et al.*, 2018 Stress-responsive and metabolic gene regulation are altered in low S-adenosylmethionine. *PLoS Genet.* 14: e1007812. <https://doi.org/10.1371/journal.pgen.1007812>
- Eden, E., R. Navon, I. Steinfeld, D. Lipson, and Z. Yakhini, 2009 GOrilla: a tool for discovery and visualization of enriched GO terms in ranked gene lists. *BMC Bioinformatics* 10: 48. <https://doi.org/10.1186/1471-2105-10-48>
- Eisen, M. B., P. T. Spellman, P. O. Brown, and D. Botstein, 1998 Cluster analysis and display of genome-wide expression patterns. *Proc. Natl. Acad. Sci. USA* 95: 14863–14868. <https://doi.org/10.1073/pnas.95.25.14863>
- Fire, A., S. Xu, M. K. Montgomery, S. A. Kostas, S. E. Driver *et al.*, 1998 Potent and specific genetic interference by double-stranded RNA in *Caenorhabditis elegans*. *Nature* 391: 806–811. <https://doi.org/10.1038/35888>
- Graham, P. L., J. J. Johnson, S. Wang, M. H. Sibley, M. C. Gupta *et al.*, 1997 Type IV collagen is detectable in most, but not all, basement membranes of *Caenorhabditis elegans* and assembles on tissues that do not express it. *J. Cell Biol.* 137: 1171–1183. <https://doi.org/10.1083/jcb.137.5.1171>
- Greenstein, D., 2005 Control of oocyte meiotic maturation and fertilization (December 28, 2005), *WormBook*, ed. The *C. elegans* Research Community, WormBook, doi/10.1895/wormbook.1.53.1, <http://www.wormbook.org>
- Hansen, M., A. L. Hsu, A. D. Dillin, and C. Kenyon, 2005 New genes tied to endocrine, metabolic, and dietary regulation of lifespan from a *Caenorhabditis elegans* genomic RNAi screen. *PLoS Genet.* 1: 119–128. <https://doi.org/10.1371/journal.pgen.0010017>
- Hillier, L. W., A. Coulson, J. I. Murray, Z. Bao, J. E. Sulston *et al.*, 2005 Genomics in *C. elegans*: so many genes, such a little worm. *Genome Res.* 15: 1651–1660. <https://doi.org/10.1101/gr.3729105>
- Hubbard, E. J., and D. Greenstein, 2005 Introduction to the germ line (September 1, 2005), *WormBook*, ed. The *C. elegans* Research Community, WormBook, doi/10.1895/wormbook.1.18.1, <http://www.wormbook.org>
- Inglis, P. N., G. Ou, M. R. Leroux, and J. M. Scholey, 2007 The sensory cilia of *Caenorhabditis elegans* (March 8, 2007), *WormBook*, ed. The *C. elegans* Research Community, WormBook, doi/10.1895/wormbook.1.126.2, <http://www.wormbook.org>
- Kaletsky, R., V. Yao, A. Williams, A. M. Runnels, A. Tadych *et al.*, 2018 Transcriptome analysis of adult *Caenorhabditis elegans* cells reveals tissue-specific gene and isoform expression. *PLoS Genet.* 14: e1007559. <https://doi.org/10.1371/journal.pgen.1007559>
- Kamath, R. S., A. G. Fraser, Y. Dong, G. Poulin, R. Durbin *et al.*, 2003 Systematic functional analysis of the *Caenorhabditis elegans* genome using RNAi. *Nature* 421: 231–237. <https://doi.org/10.1038/nature01278>
- Krämer, A., J. Green, J. Pollard, Jr., and S. Tugendreich, 2014 Causal analysis approaches in ingenuity pathway analysis. *Bioinformatics* 30: 523–530. <https://doi.org/10.1093/bioinformatics/btt703>
- LaMacchia, J. C., H. N. Frazier, III, and M. B. Roth, 2015 Glycogen fuels survival during hypotonic-anoxic stress in *Caenorhabditis elegans*. *Genetics* 201: 65–74. <https://doi.org/10.1534/genetics.115.179416>
- Lee, M. H., and T. Schedl, 2006 RNA-binding proteins (April 18, 2006), *WormBook*, ed. The *C. elegans* Research Community, WormBook, doi/10.1895/wormbook.1.79.1, <http://www.wormbook.org>
- Lee, R. Y. N., K. L. Howe, T. W. Harris, V. Arnaboldi, S. Cain *et al.*, 2018 WormBase 2017: molting into a new stage. *Nucleic Acids Res.* 46: D869–D874. <https://doi.org/10.1093/nar/gkx998>
- EHernault, S. W., 2006 Spermatogenesis (February 20, 2006), *WormBook*, ed. The *C. elegans* Research Community, WormBook, doi/10.1895/wormbook.1.85.1, <http://www.wormbook.org>
- Li, C., and K. Kim, 2008 Neuropeptides (September 25, 2008), *WormBook*, ed. The *C. elegans* Research Community, WormBook, doi/10.1895/wormbook.1.142.1, <http://www.wormbook.org>
- MacNeil, L. T., E. Watson, H. E. Arda, L. J. Zhu, and A. J. M. Wallhout, 2013 Diet-induced developmental acceleration independent of TOR and insulin in *C. elegans*. *Cell* 153: 240–252. <https://doi.org/10.1016/j.cell.2013.02.049>
- Marchler-Bauer, A., Y. Bo, L. Han, J. He, C. J. Lanczycki *et al.*, 2017 CDD/SPARCLE: functional classification of proteins via subfamily domain architectures. *Nucleic Acids Res.* 45: D200–D203. <https://doi.org/10.1093/nar/gkw1129>
- Mato, J. M., and S. C. Lu, 2007 Role of S-adenosyl-L-methionine in liver health and injury. *Hepatology* 45: 1306–1312. <https://doi.org/10.1002/hep.21650>
- McDonald, J. H., 2014 *Handbook of Biological Statistics*. Sparky House Publishing, Baltimore.
- Mi, H., A. Muruganujan, X. Huang, D. Ebert, C. Mills *et al.*, 2019 Protocol Update for large-scale genome and gene function analysis with the PANTHER classification system (v.14.0). *Nat. Protoc.* 14: 703–721. <https://doi.org/10.1038/s41596-019-0128-8>
- Murphy, C. T., S. A. McCarroll, C. I. Bargmann, A. Fraser, R. S. Kamath *et al.*, 2003 Genes that act downstream of DAF-16 to influence the lifespan of *Caenorhabditis elegans*. *Nature* 424: 277–283. <https://doi.org/10.1038/nature01789>
- Oliveira, R. P., J. Porter Abate, K. Dilks, J. Landis, J. Ashraf *et al.*, 2009 Condition-adapted stress and longevity gene regulation by *Caenorhabditis elegans* SKN-1/Nrf. *Aging Cell* 8: 524–541. <https://doi.org/10.1111/j.1474-9726.2009.00501.x>
- Ortiz, M. A., D. Noble, E. P. Sorokin, and J. Kimble, 2014 A new dataset of spermatogenic vs. oogenic transcriptsomes in the nematode *Caenorhabditis elegans*. *G3 (Bethesda)* 4: 1765–1772. <https://doi.org/10.1534/g3.114.012351>
- Reinke, V., H. E. Smith, J. Nance, J. Wang, C. Van Doren *et al.*, 2000 A global profile of germline gene expression in *C. elegans*. *Mol. Cell* 6: 605–616. [https://doi.org/10.1016/S1097-2765\(00\)00059-9](https://doi.org/10.1016/S1097-2765(00)00059-9)
- Ritter, A. D., Y. Shen, J. Fuxman Bass, S. Jeyaraj, B. Deplancke *et al.*, 2013 Complex expression dynamics and robustness in *C. elegans* insulin networks. *Genome Res.* 23: 954–965. <https://doi.org/10.1101/gr.150466.112>
- Robertson, H. M., and J. H. Thomas, 2006 The putative chemoreceptor families of *C. elegans* (January 06, 2006), *WormBook*, ed. The *C. elegans* Research Community, WormBook, doi/10.1895/wormbook.1.66.1, <http://www.wormbook.org>
- Rual, J. F., J. Ceron, J. Koreth, T. Hao, A. S. Nicot *et al.*, 2004 Toward improving *Caenorhabditis elegans* phenome mapping with an ORFeome-based RNAi library. *Genome Res.* 14: 2162–2168. <https://doi.org/10.1101/gr.2505604>
- Schwarz, E. M., M. Kato, and P. W. Sternberg, 2012 Functional transcriptomics of a migrating cell in *Caenorhabditis elegans*. *Proc. Natl. Acad. Sci. USA* 109: 16246–16251. <https://doi.org/10.1073/pnas.1203045109>
- Smulan, L. J., W. Ding, E. Freinkman, S. Gujja, Y. J. Edwards *et al.*, 2016 Cholesterol-independent SREBP-1 maturation is linked to ARF1 inactivation. *Cell Rep.* 16: 9–18. <https://doi.org/10.1016/j.celrep.2016.05.086>

- Spellman, P. T., G. Sherlock, M. Q. Zhang, V. R. Iyer, K. Anders *et al.*, 1998 Comprehensive identification of cell cycle-regulated genes of the yeast *Saccharomyces cerevisiae* by microarray hybridization. *Mol. Biol. Cell* 9: 3273–3297. <https://doi.org/10.1091/mbc.9.12.3273>
- Spencer, W. C., G. Zeller, J. D. Watson, S. R. Henz, K. L. Watkins *et al.*, 2011 A spatial and temporal map of *C. elegans* gene expression. *Genome Res.* 21: 325–341. <https://doi.org/10.1101/gr.114595.110>
- Supek, F., M. Bosnjak, N. Skunca, and T. Smuc, 2011 REVIGO summarizes and visualizes long lists of gene ontology terms. *PLoS One* 6: e21800. <https://doi.org/10.1371/journal.pone.0021800>
- The Gene Ontology Consortium, 2019 The gene ontology resource: 20 years and still GOing strong. *Nucleic Acids Res.* 47: D330–D338. <https://doi.org/10.1093/nar/gky1055>
- Vance, D. E., 2014 Phospholipid methylation in mammals: from biochemistry to physiological function. *Biochim. Biophys. Acta* 1838: 1477–1487. <https://doi.org/10.1016/j.bbamem.2013.10.018>
- Varkey, J. P., P. L. Jansma, A. N. Minniti, and S. Ward, 1993 The *Caenorhabditis elegans spe-6* gene is required for major sperm protein assembly and shows second site non-complementation with an unlinked deficiency. *Genetics* 133: 79–86.
- Walker, A. K., R. L. Jacobs, J. L. Watts, V. Rottiers, K. Jiang *et al.*, 2011 A conserved SREBP-1/phosphatidylcholine feedback circuit regulates lipogenesis in metazoans. *Cell* 147: 840–852. <https://doi.org/10.1016/j.cell.2011.09.045>
- Watts, J. L., and M. Ristow, 2017 Lipid and carbohydrate metabolism in *Caenorhabditis elegans*. *Genetics* 207: 413–446.
- Xu, W., L. Yi, Y. Feng, L. Chen, and J. Liu, 2009 Structural insight into the activation mechanism of human pancreatic phospholipase A2. *J. Biol. Chem.* 284: 16659–16666. <https://doi.org/10.1074/jbc.M808029200>

*Communicating editor: V. Reinke*